

Supplementary Information

Selectively activated suppressed quantum networks in self-assembled single atom-Ag catalyst-based room temperature sensors for health monitoring

Nirman Chakraborty,^{1,2*} Anagha Ghosh,² Subhajit Mojumder,² Ajay K. Mishra^{3,4} and Swastik Mondal^{2,5*}

¹Schulich Faculty of Chemistry, Solid State Institute, Technion-Israel Institute of Technology, Haifa 3200003, Israel

²CSIR-Central Glass and Ceramic Research Institute, 196, Raja S. C. Mullick Road, Jadavpur, Kolkata 700032, India

³High Pressure and Synchrotron Radiation Physics Division, Bhabha Atomic Research Centre, Trombay, Mumbai 400085, India

⁴Homi Bhabha National Institute, DAE, Anushaktinagar, Mumbai 400094, India

⁵Academy of Scientific and Innovative Research (AcSIR), Ghaziabad 201002, India

*Corresponding author: nirman-c@campus.technion.ac.il; swastik_mondal@cgcri.res.in

Contents

1. Synthesis of CdO as precursor and analyses of intermediate stages of CdS QD formation
2. Electron microscopic studies
3. XPS analyses
4. XANES results
5. Hall configuration
6. Sensing results
7. PL measurements
8. UV Vis spectroscopy
9. Ohmic characteristic analysis
10. Control experiment schematic
11. Impedance spectra

1. Synthesis of CdO as precursor and analyses of intermediate stages of CdS QD formation

CdO was synthesized by a standard precipitation technique.¹ In this method, a 1.0M solution of $\text{Cd}(\text{NO}_3)_2 \cdot 4\text{H}_2\text{O}$ was prepared in DI water and ammonia solution was added dropwise till a yellowish precipitate was formed at pH 9. The mixture was centrifuged in wash ethanol medium to remove unreacted components and then dried at 60°C for 6 hours. The sample was then calcined at 400°C for 5 hours and ground finely to obtain a brownish powder. The sample was checked for formation of phase pure CdO by powder XRD.¹

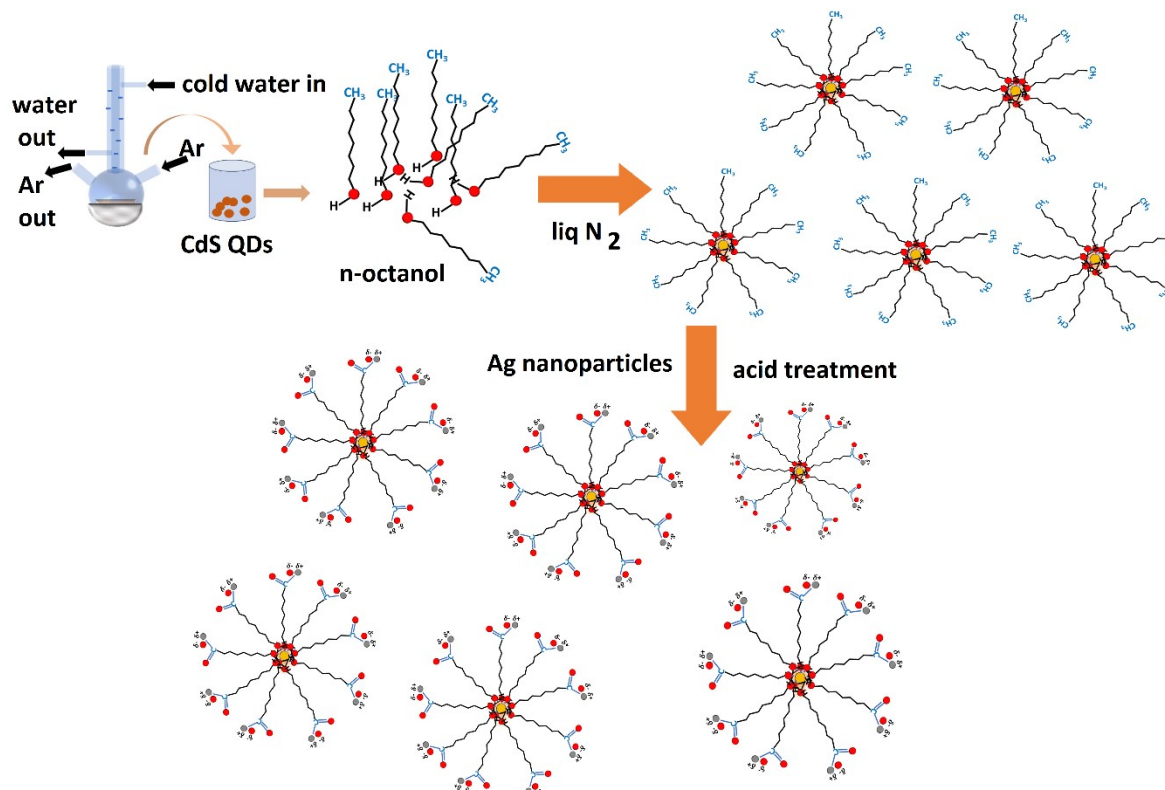


Figure S1: Schematic of the n-octanol assembly on CdS QDs and subsequent conversion to Ag@n-octanol(ox)@CdS QD assembly.

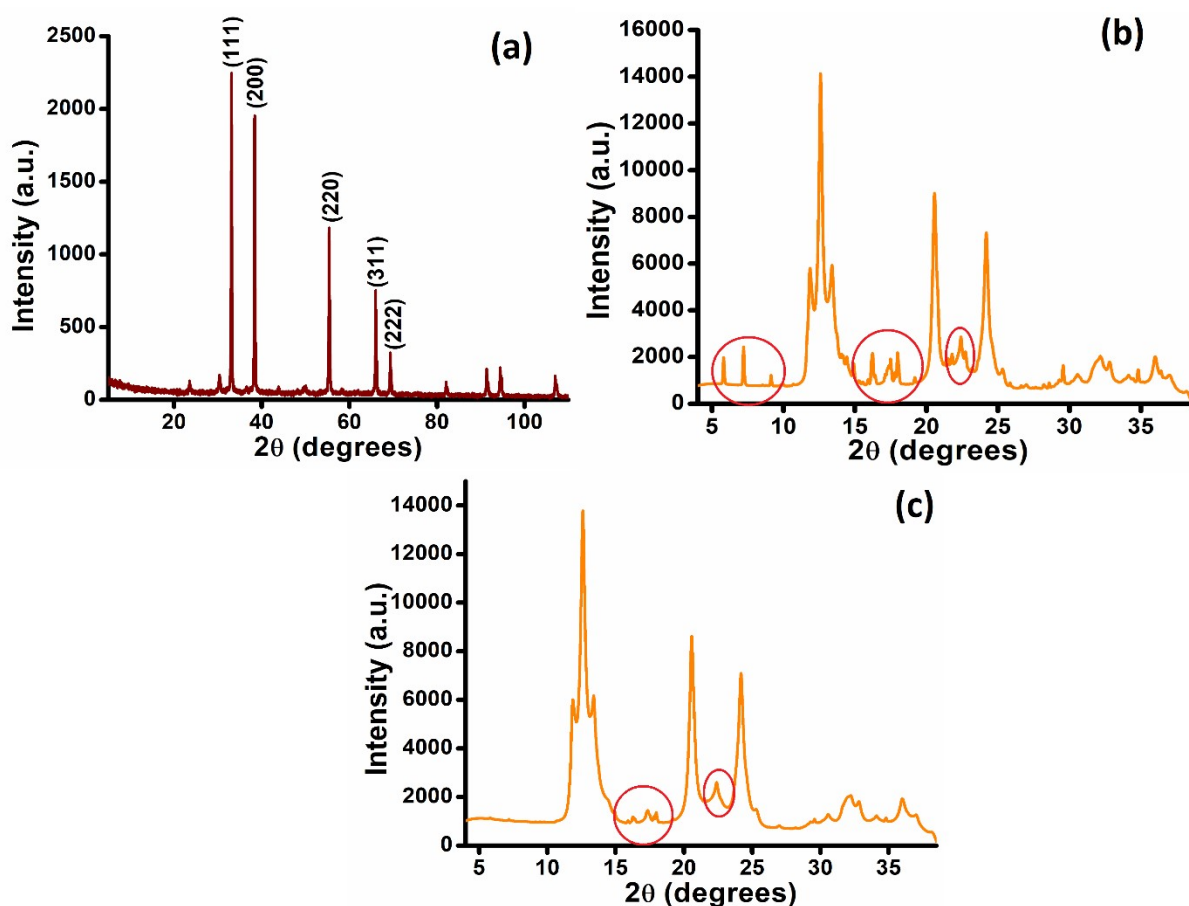


Figure S2: (a) Room temperature powder XRD of synthesized CdO for CdS QD preparation. (b-c) XRD patterns at intermediate stages of CdS QD formation with additional peaks highlighted in red circles.

Table S1: Ag precursor concentration vs. amount settled on the n-octanol(ox) substrate.

Sl. No.	Composition name	Ag solution (ml)	Ag:CdS (TEM EDX)
1	Ag@n-octanol(ox)@CdS QD_1	20	7%
2	Ag@n-octanol(ox)@CdS QD_2	40	4%
3	Ag@n-octanol(ox)@CdS QD_3	60	3.9%
4	Ag@n-octanol(ox)@CdS QD_4	80	4.1%

2. Electron microscopic studies

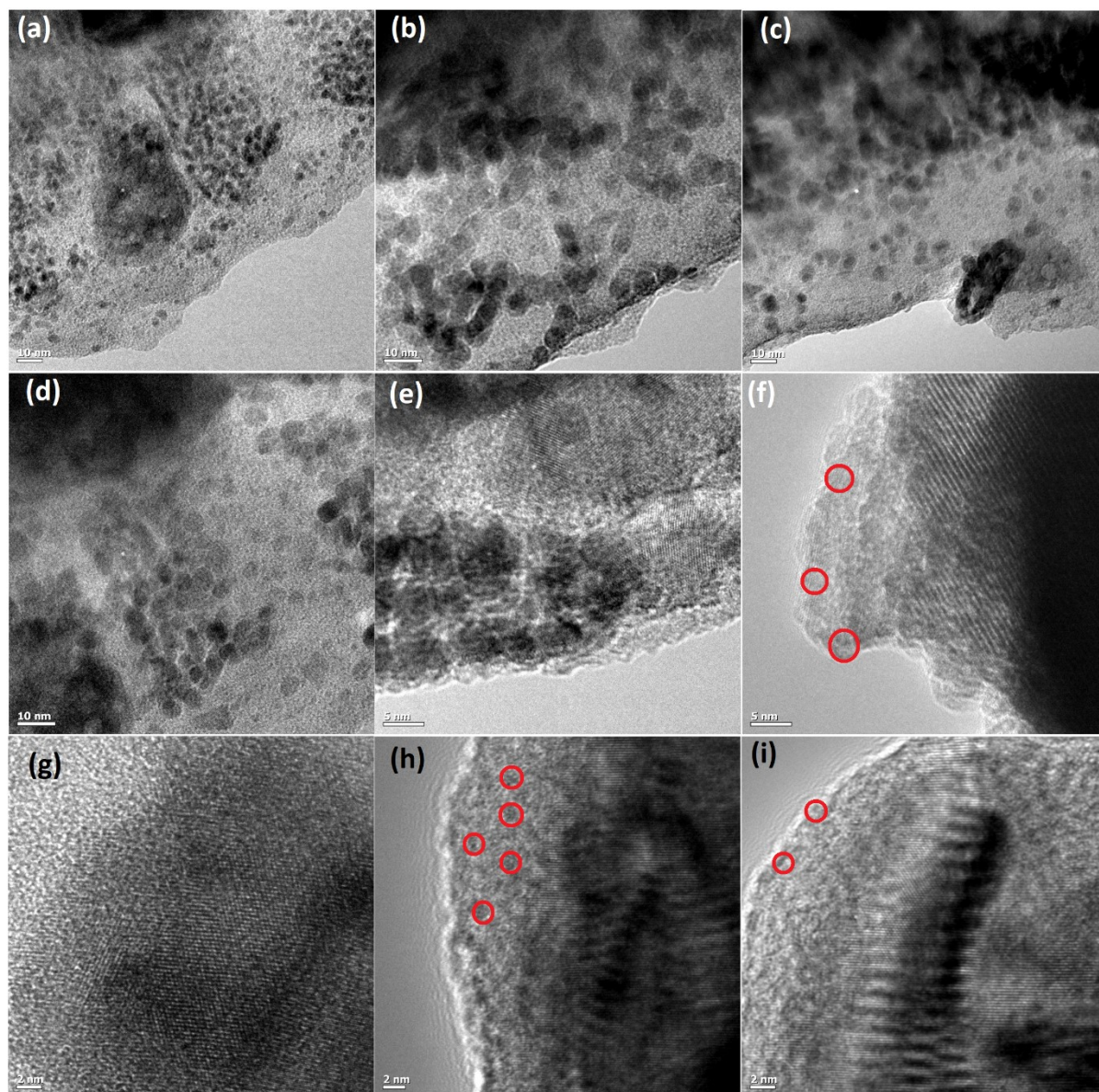


Figure S3: (a-c) Bright field TEM image of n-octanol@CdS QD assembly (d-e) Ag@n-octanol(ox)@CdS QD assembly (f-i) HRTEM images of Ag@n-octanol(ox)@CdS QD assembly with Ag highlighted in red circles.

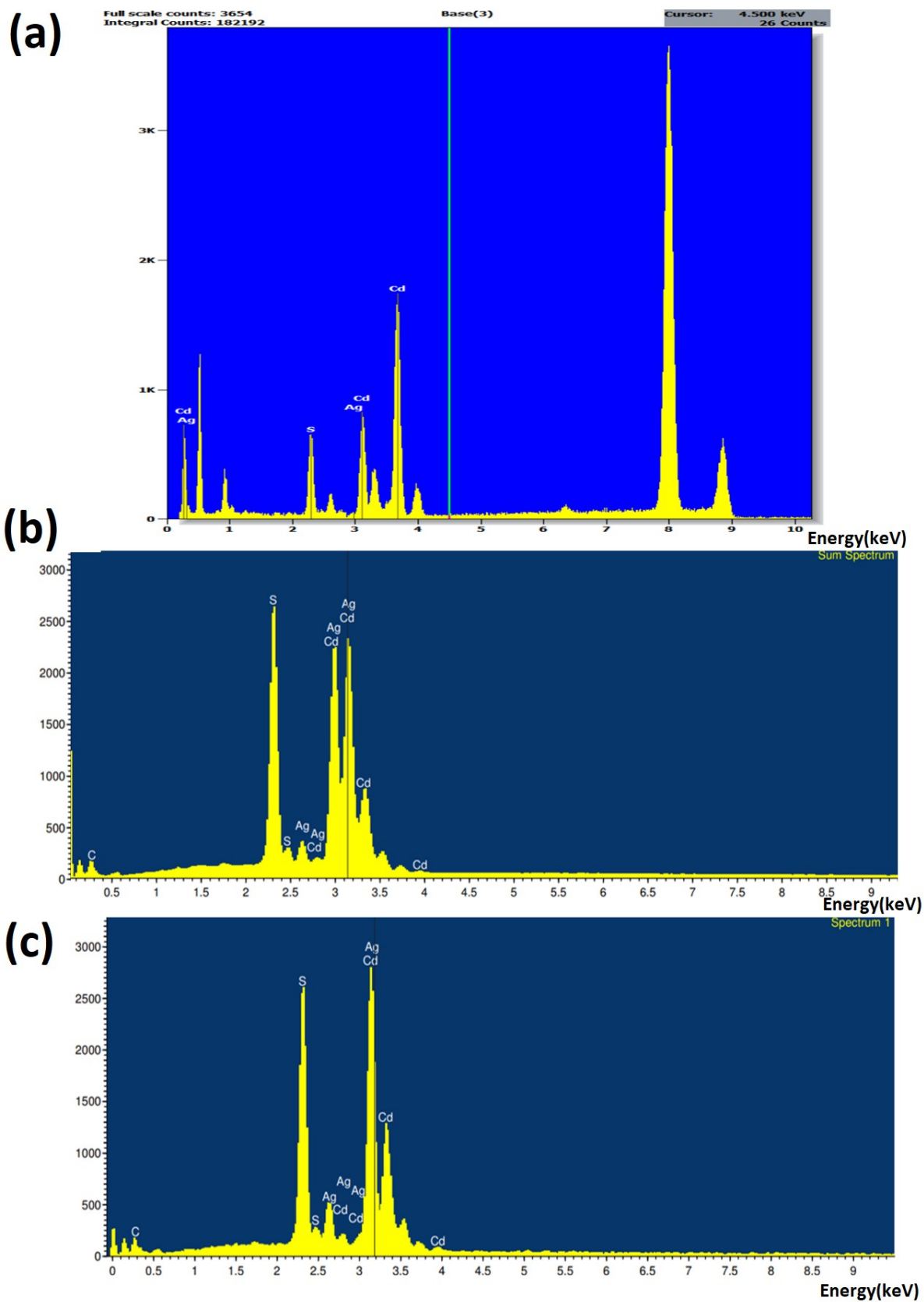


Figure S4: (a) TEM EDX spectrum of Ag@n-octanol(ox)@CdS QD₁ assembly with 7% Ag@CdS (w/w) (b-c) SEM EDX spectra of Ag@n-octanol(ox)@CdS QD₁ and Ag@n-

octanol(ox)@CdS QD_2 assembly with 7% Ag@CdS and 4% Ag@CdS (w/w) respectively. The spectra are taken from an average of 3 spots on the sample mounted.

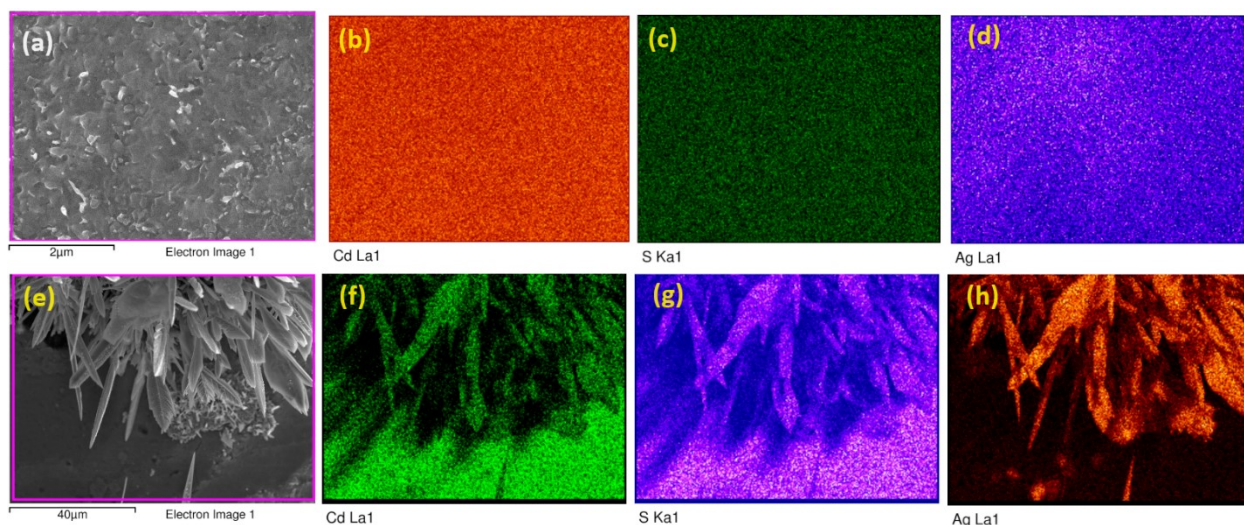


Figure S5: SEM color mapping of two different regions of the Ag@n-octanol(ox)@CdS QD_1 sample [(b-d) for region (a) and (f-h) for region (e)].

3. XPS analyses

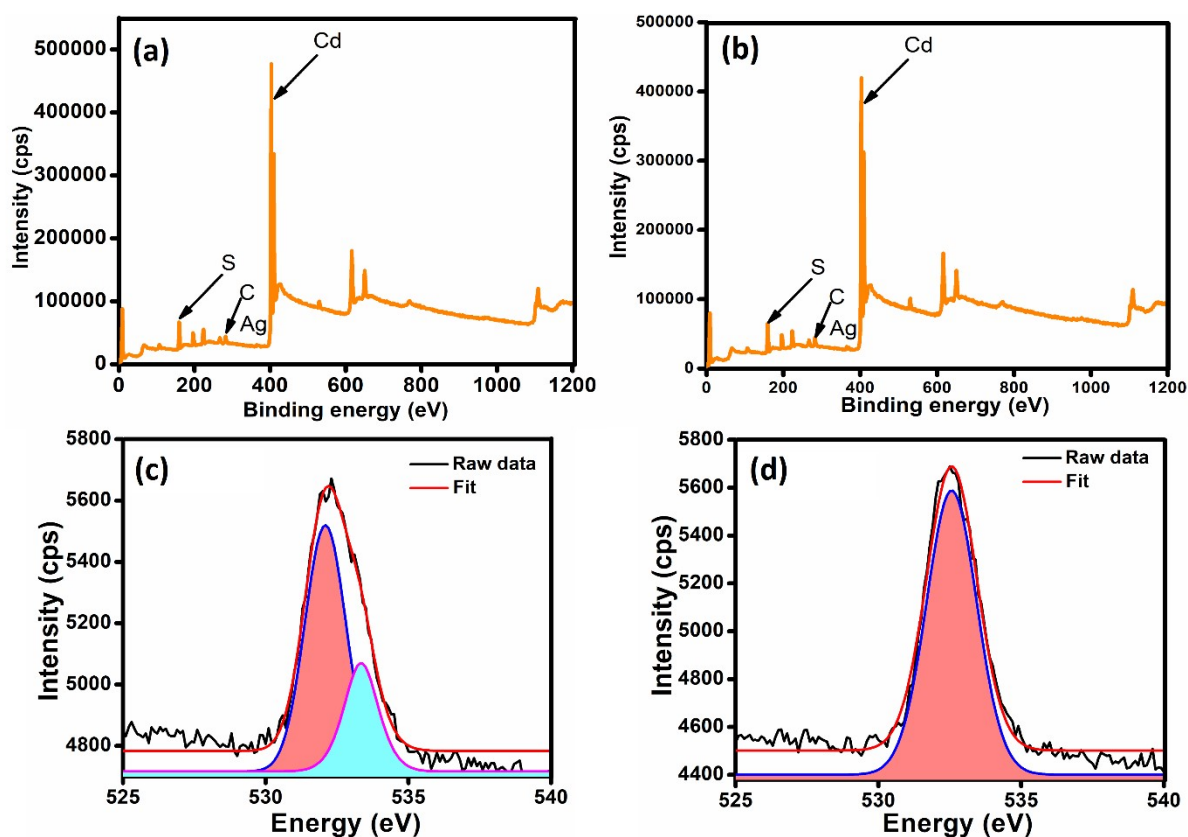


Figure S6: (a-b) Survey scan of Ag@n-octanol(ox)@CdS QD_1 and Ag@n-octanol(ox)@CdS QD_2 assembly with specific elements marked. (c-d) O1s core level spectra of Ag@n-octanol(ox)@CdS QD_2 and Ag@n-octanol(ox)@CdS QD_1 assembly. In (c) pink peak refers to O of -C=O and blue the surface hydroxyl groups. In (d) the O of -C=O

is prominent, but the hydroxyl signal gets hidden probably due to greater conversion of -OH^+ to $\text{-O}^-\text{Ag}^+$.²

4. XANES results

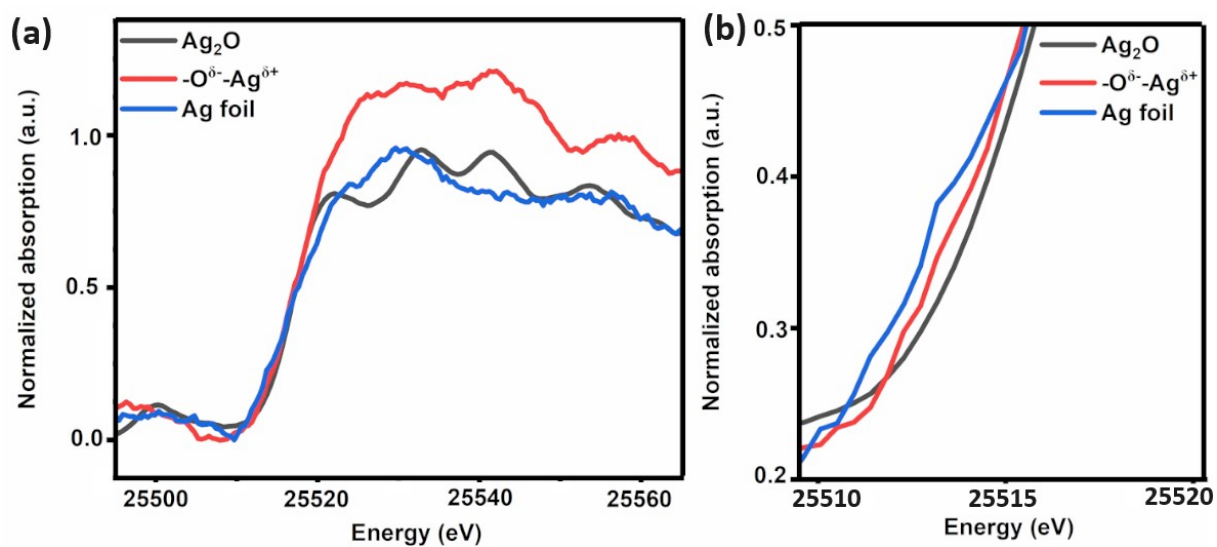


Figure S7: Ag K-edge XANES of (a) Ag foil, Ag₂O, Ag@n-octanol(ox)@CdS QD_1 (b) Enlarged region from 25.510 keV to 25.515 keV showing the edge for Ag@n-octanol(ox)@CdS QD_1 lying between Ag foil and Ag₂O.

5. Hall configuration

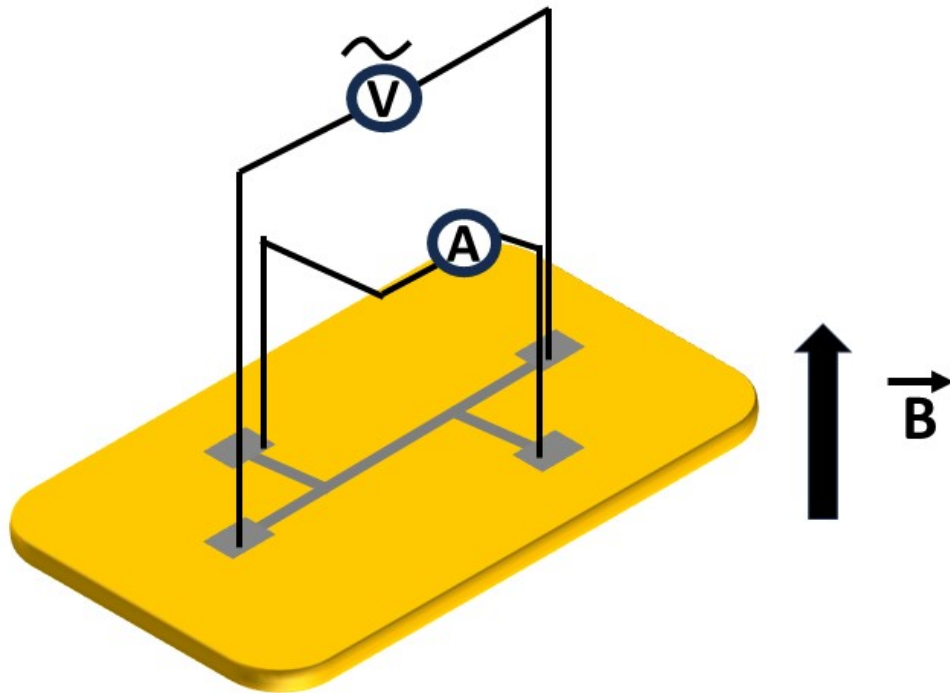


Figure S8: 4-probe Hall configuration of the sample.³ V represents the voltage source and A the current meter. B is the applied magnetic field in a direction perpendicular to the sample plane. The grey lines are for representation purposes. The square contacts are made of silver. The length of the common is $l = 2.3$ mm and thickness of the pellet is $d = 5$ mm. 4-probe

resistivity has been calculated by standard formula of $R = \rho \frac{l}{A}$ where R is the resistance, ρ is the resistivity, l is the length of common region and A is the cross-sectional area $A = l \times d$.

6. Sensing results

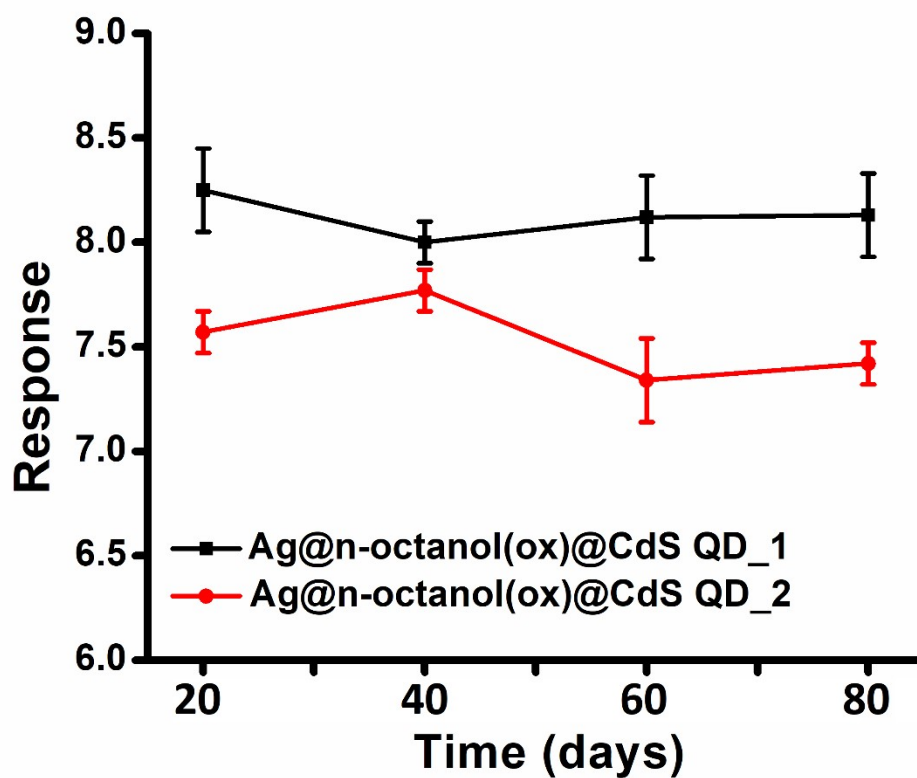


Figure S9: Repeatability of sensor samples with time for 500 ppb ethanol at room temperature.

7. PL measurements

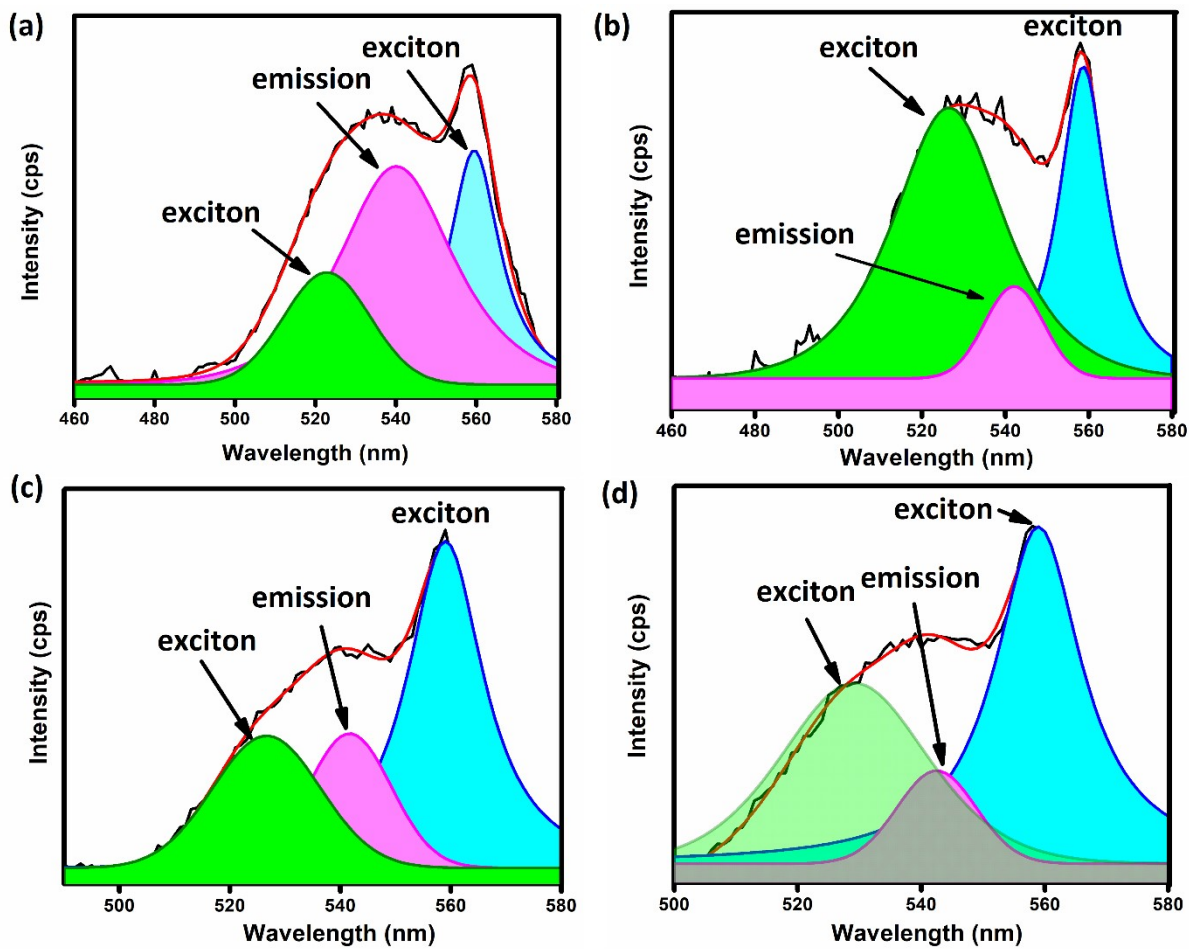


Figure S10: Low temperature PL spectra (78K) of (a) CdS QD (b) n-octanol@CdS QD, (c) Ag@n-octanol(ox)@CdS_1 and (d) Ag@n-octanol(ox)@CdS_2 samples respectively.

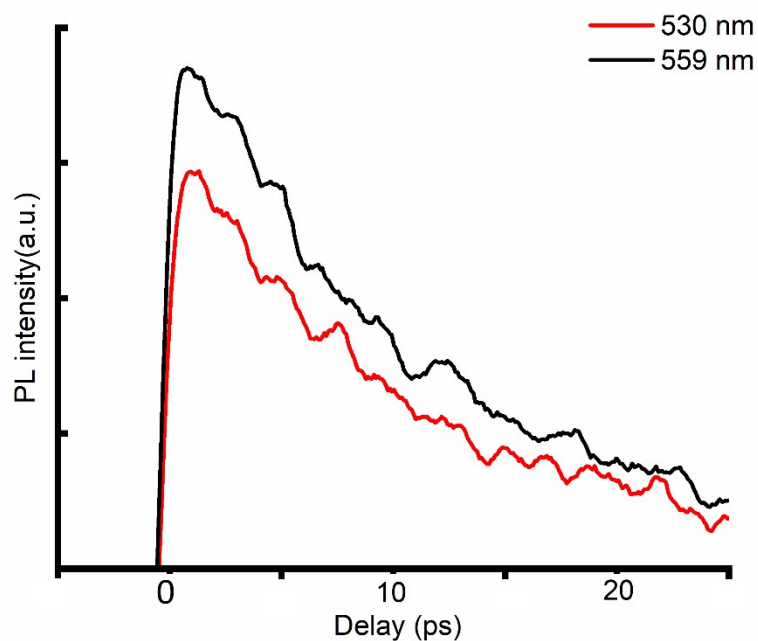


Figure S11: Lifetime measurement (78 K) of 530 nm emission and 559 nm emission in Ag@n-octanol(ox)@CdS_1 sample.

8. UV Vis spectroscopy

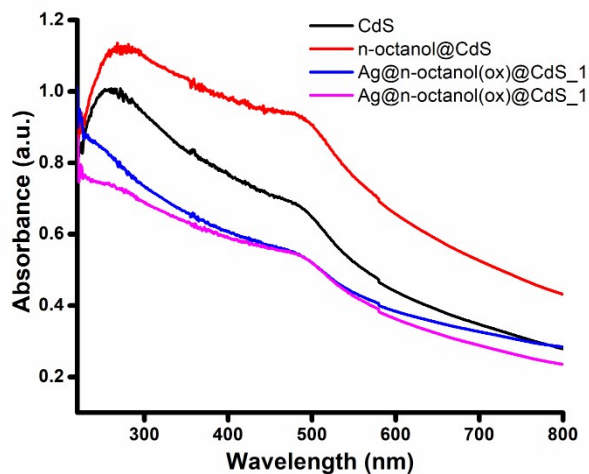


Figure S12: Room temperature UV Vis spectra of all samples in iso-propanol medium.

9. Ohmic characteristic analysis

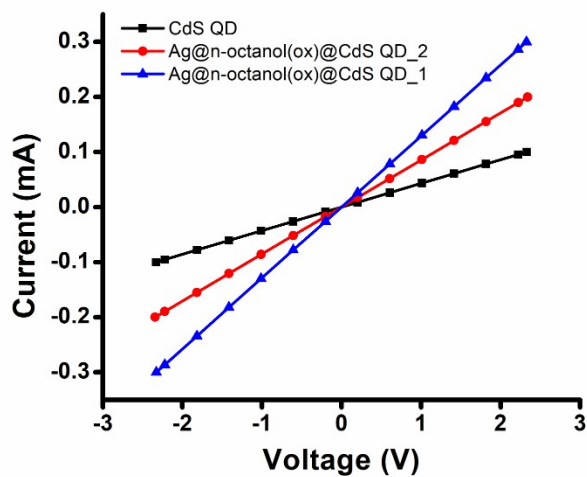


Figure S13: Room temperature I-V characteristics of sensor samples showing the ohmic nature of the sensors.

10. Control experiment schematic

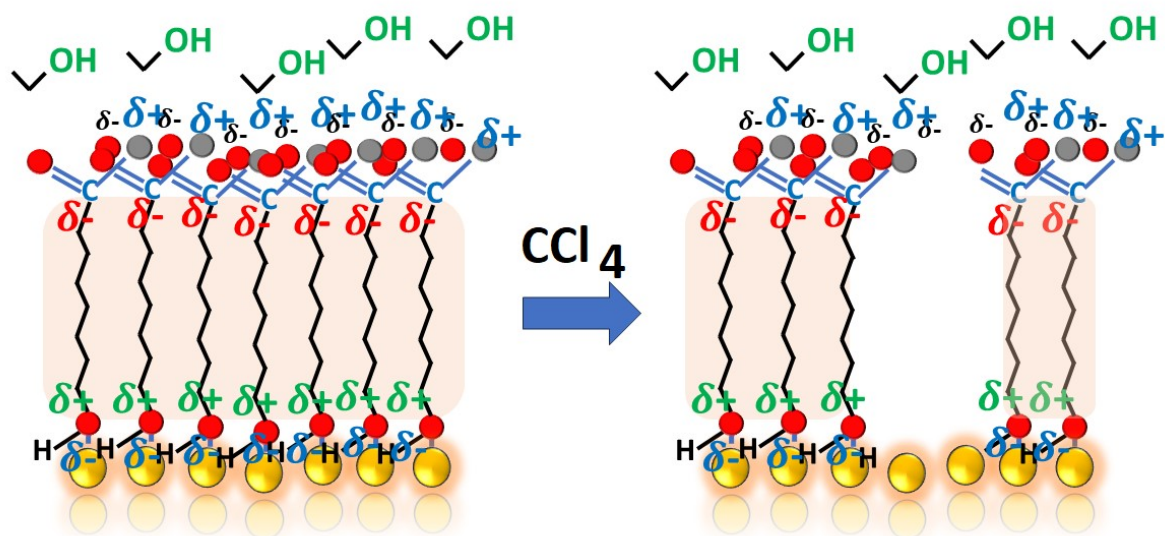


Figure S14: A small dent made on the encapsulation using CCl_4 .⁴ The capacitance measured was $1.5 \mu\text{F}$ with dissipation of 50%.

11. Impedance spectra

(i)

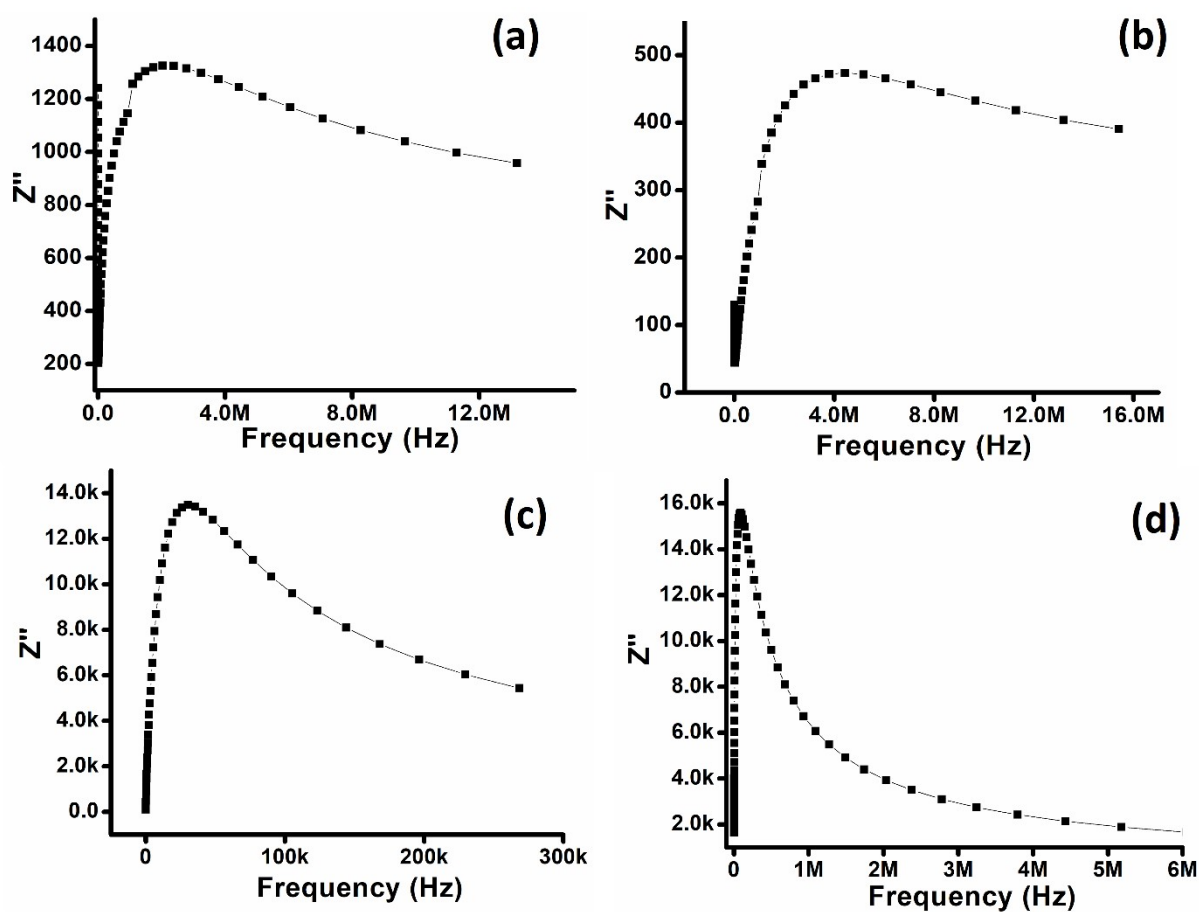


Figure S15: Capacitive reactance of (a, c) Ag@n-octanol(ox)@CdS_1 and (b, d) Ag@n-octanol(ox)@CdS_2 samples respectively in absence and presence of 200 ppm ethanol after 45 minutes of interaction

(ii)

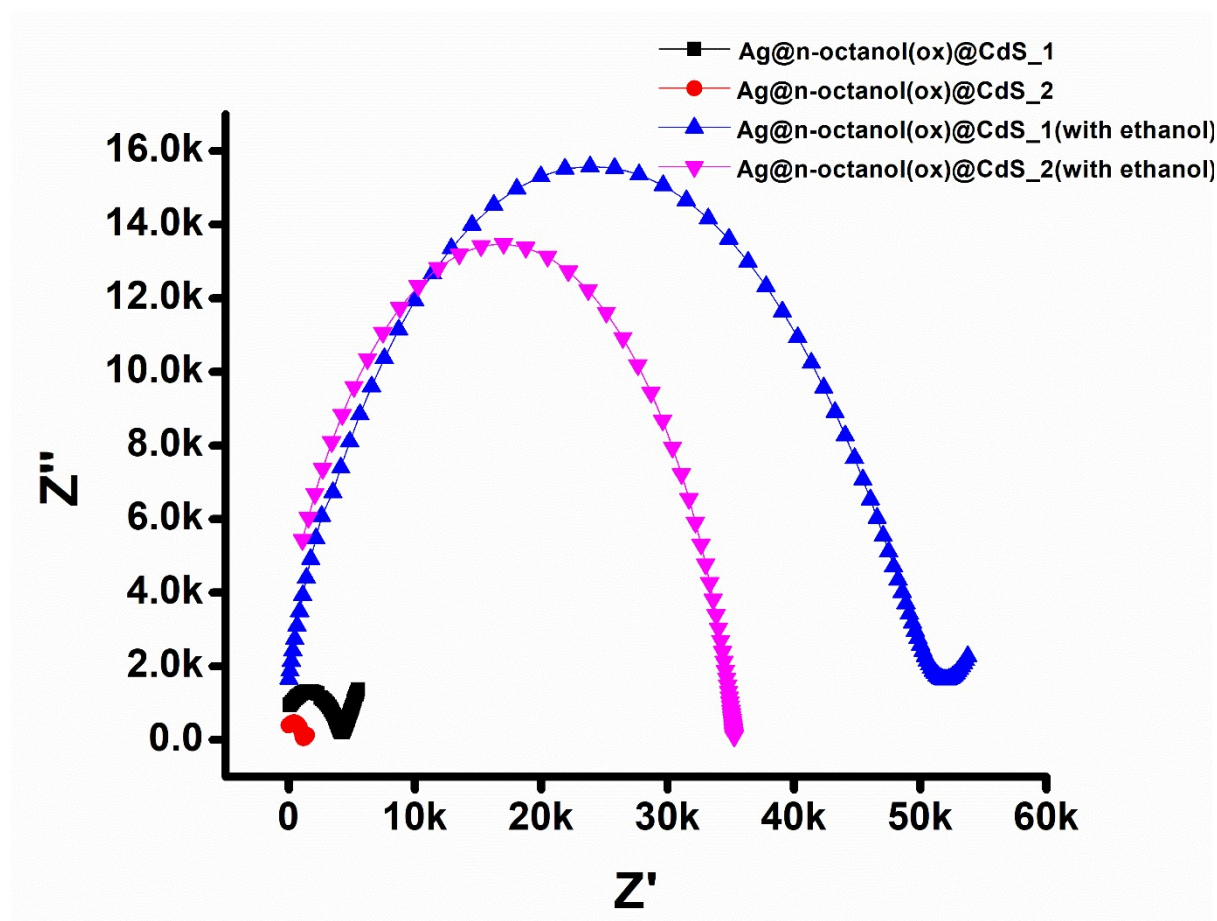


Figure S16: Nyquist plots⁵ for the SACs in presence and absence of ethanol.

References

1. M. Ahmed, S. Mukherjee, T. Singha, P.M.G. Nambissan Defect characteristics of cadmium oxide nanocrystallites synthesized via a chemical precipitation method. *Journal of Physics and Chemistry of Solids* 181 (2023) 111513.
2. Q.T. Le, E. Gül Arslan, J. Rip, H. De Coster, P. Verdonck, D. Radisic, F. Schleicher, I. Vaesen, T. Conard, E. Altamirano-Sanchez Studying the efficacy of hydrogen plasma treatment for enabling the etching of thermally annealed ruthenium in chemical solutions. *Micro and Nano Engineering* 19 (2023) 100208.
3. B. Guralnik¹, O. Hansen, A. R. Stilling-Andersen, S. E. Hansen, K. A. Borup, B. M. Mihiretie, B. Beltrán-Pitarch, H. H. Henrichsen, R. Lin, L. Shiv, B. B. Iversen, P. F. Nielsen and D. H. Petersen Determination of thermoelectric properties from micro four-point probe measurements. *Meas. Sci. Technol.* 33 (2022) 125001.
4. <https://pubchem.ncbi.nlm.nih.gov/compound/1-Octanol>

5. BA. Mei, O. Munteshari, J. Lau, B. Dunn, and L. Pilon Physical Interpretations of Nyquist Plots for EDLC Electrodes and Devices. *J. Phys. Chem. C* 122 (2018) 194–206.